

A Novel Approach for the Synthesis and Characterization Studies of Mn^{2+} -Doped CdS Nanocrystals by a Facile Microwave-Assisted Combustion Method

A. Manikandan · S. Arul Antony

Received: 7 July 2014 / Accepted: 18 July 2014 / Published online: 3 September 2014
© Springer Science+Business Media New York 2014

Abstract A simple and efficient microwave-assisted combustion method was developed to synthesize Mn^{2+} -doped CdS ($\text{Mn}_x\text{Cd}_{1-x}\text{S}$; $x = 0.0, 0.3, \text{ and } 0.5$) nanocrystallites. The study suggested that the application of microwave heating produced spherical shaped cluster of pure and Mn^{2+} -doped CdS nanocrystallites, which was achieved in few minutes. The effects of Mn^{2+} -doping on structural, morphological, optical and magnetic properties of CdS nanocrystallites were investigated by powder X-ray diffraction (XRD), Fourier transform infrared spectroscopy (FT-IR), high-resolution scanning electron microscopy (HR-SEM) with energy dispersive X-ray analysis (EDX), high-resolution transmission electron microscopy (HR-TEM) with selected area electron diffraction (SAED), UV-Visible diffuse reflectance spectroscopy (DRS), photoluminescence (PL) spectroscopy, and vibrating sample magnetometer (VSM). The XRD results confirmed the formation of hexagonal CdS. The formation of pure and Mn^{2+} -doped CdS phase was also confirmed by FT-IR and EDX. The formation of spherical shaped cluster of nanocrystallites was confirmed by HR-SEM and HR-TEM. The as-synthesized nanocrystallites were found to have good optoelectronic properties that were determined by DRS and PL spectra. VSM results of the as-synthesized Mn^{2+} -doped CdS nanocrystallites showed ferromagnetic behavior.

Keywords CdS nanocrystals · Combustion method · Electron microscopy · Magnetic properties · Optical properties · X-ray diffraction

1 Introduction

Generally, nanostructured materials are of both fundamental and industrial attention for their interesting and potentially useful structural, physical, and chemical properties. Nanocrystalline semiconducting materials are important in technological and industrial applications, due to their unusual physicochemical properties than those of their bulk counterparts. Over the past few years, a variety of oxides (ZnO [1, 2], SnO_2 [3], Ga_2O_3 [4], In_2O_3 [5], Fe_2O_3 [6], and Co_3O_4 [7]), nitride (GaN [8]), and sulfide (ZnS [9] and CdS [10–13]) nanostructures have been reported. Among them, cadmium sulfide, CdS, is an important II–IV group semiconducting materials with a direct bandgap E_g of 2.42 eV at room temperature and can be widely used for a host of applications in optoelectronics, such as nonlinear optics, flat panel displays, light-emitting diodes, lasers, thin-film transistors, etc. [14, 15]. Since the properties of nano-materials mainly depend on the morphological features, a variety of CdS nanostructures have been synthesized including nanowires, nanorods, nanotubes, hollow sphere, peanut, and nanocable by various physical and chemical methods [16–20]. Various approaches such as solvothermal [21], liquid crystal template [22], irradiation [23], sedimentation [24], thermal evaporation [25], polymer-controlled growth [16], and electrodeposition on a porous template [26] have been applied to achieve CdS nanocrystals. In these methods, sophisticated equipments, difficulty in preparation, and economically prohibitive high temperatures are usually required. However, it is inevitable to use template and

A. Manikandan (✉) · S. Arul Antony
PG and Research Department of Chemistry, Presidency College
(Autonomous), Chennai 600 005, India
e-mail: mkavath15@gmail.com

S. Arul Antony
e-mail: antonypresidency15@gmail.com

high temperature or catalyst in the synthesis process, which seemed to be of less advantage and with low economically viable processes for the preparation of CdS nanostructures.

However, microwave-assisted combustion method is a novel method to produce nanocrystalline materials, since microwave heating is an in situ mode of energy conversion and is fundamentally different from conventional heating processes. When a liquid is exposed to microwave radiation, the microwaves induce rotation of the dipoles within the liquid and electromagnetic radiations, which causes the liquid to become hot. Thus, the heat is produced within the liquid and not transferred from the vessel as in other conventional systems. The efficient way of localized heating has been reported [27] to lead to increase in reaction rates, yield, and improvement of the product formation. Thus, low temperature and fast growth synthesis of II–VI semiconductor nanocrystalline materials are a major consideration of current research.

Recently, doped semiconductor nanomaterials are being studied intensively to achieve two different material properties, such as optical and magnetic properties. If the doping atoms have unfilled d electrons, then one also observes the magnetic properties. In this present study, Mn^{2+} -doped CdS nanocrystals have been mainly studied, due to their optical and magnetic properties. CdS has two different crystal patterns, namely cubic and hexagonal. As we know, cubic CdS is in metastable phase, while hexagonal CdS is the thermodynamically stable semiconductor. Usually, it was believed that the phase transition process of CdS from cubic to hexagonal would happen under high temperature [28]. Investigations on different scale nanostructures and respective morphologies of CdS are still warranted. To the best of our knowledge, the preparation of CdS nanocrystallites by microwave combustion method has rarely been reported so far. Murugan et al. [27] reported the formation of CdS nanorods and nanoparticles by microwave method, and Thongtem et al. [29] reported the nano- and microcrystalline CdS using cyclic microwave radiation. Both methods are complicated, time-consuming, and require double-walled digestion vessels consisting of a Teflon (TFM) inner liner. Nag et al. [30] have reported luminescence properties in Mn-doped CdS nanocrystals, and the preparation procedure takes too long time (12 h) and needed high equipment.

Among various conventional methods of nanomaterials, microwave-assisted combustion method has been widely used to improve the crystallinity of nanostructures. Hence, in the present study, we have employed a simple, rapid, and efficient microwave-assisted combustion technique to synthesize hexagonal CdS nanocrystallites. The whole process takes only a few minutes to yield CdS nanocrystallites. The structure, morphology, optical and magnetic properties of the as-prepared pure and Mn^{2+} -doped CdS nanocrystallites were investigated by X-ray diffraction (XRD), Fourier

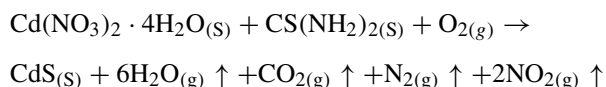
transform infrared spectroscopy (FT-IR), high-resolution scanning electron microscopy (HR-SEM), high-resolution transmission electron microscopy (HR-TEM), energy dispersive X-ray analysis (EDX), UV-Visible diffuse reflectance spectroscopy (DRS), Photoluminescence (PL) spectroscopy, and vibrating sample magnetometer (VSM) analyses.

2 Experimental Part

2.1 Preparation of Pure and Mn^{2+} -Doped CdS Nanocrystallites by a Facile Microwave-Assisted Combustion Method

All the reagents used were of Analar grade obtained from Merck, India, and were used as received without further purification. The samples were prepared with the addition of Mn^{2+} of different molar ratios ($\text{Mn}_x\text{Cd}_{1-x}\text{S}$: $x = 0.0, 0.3, \text{ and } 0.5$) to CdS. Stoichiometric amounts of cadmium nitrate, manganese nitrate, and thiourea were dissolved in deionized water and poured into a silica crucible, which was placed in a domestic microwave oven (2.45 GHz, 800 W). Initially, the solution boils and undergoes dehydration followed by decomposition with the evolution of gases. After the solution reaches the point of spontaneous combustion, it vaporizes the solution instantly and becomes a solid. The obtained solid powders was washed well with alcohol and dried. The as-prepared samples were labeled CdS, $\text{Mn}_{0.3}\text{Cd}_{0.7}\text{S}$, and $\text{Mn}_{0.5}\text{Cd}_{0.5}\text{S}$, respectively.

In general, it is believed that the reaction of cadmium nitrate salts and thiourea in the solution to produce CdS nanocrystallites has one possible route. The entire microwave-assisted combustion method produces CdS nanocrystallite powders in a microwave oven operated at a power of 800 W for 10 min. The expected combustion reaction may be as follows:



2.2 Characterizations of Pure and Mn^{2+} -Doped CdS Nanocrystallites

The structural characterization of pure and Mn^{2+} -doped CdS nanocrystallites was performed using a Philips X'pert X-ray diffractometer with $\text{CuK}\alpha$ radiation at $\lambda = 1.540 \text{ \AA}$. The surface functional groups were analyzed by Perkin Elmer FT-IR spectrometer. Morphological studies of pure and Mn^{2+} -doped CdS nanocrystallites have been performed with a Jeol JSM6360 on scanning electron microscope. The transmission electron micrographs and energy dispersive X-ray analysis were carried out by Philips-TEM (CM20).

The diffuse reflectance UV-Visible spectra of pure and Mn^{2+} -doped nanocrystallites was recorded using Cary100 UV-Visible spectrophotometer to estimate their bandgap energy. The optical properties were recorded using Varian Cary Eclipse Fluorescence Spectrophotometer. Magnetic measurements were carried out at room temperature using a PMC MicroMag 3900 model vibrating sample magnetometer (VSM) equipped with 1 T magnet.

3 Results and Discussion

3.1 X-ray Diffraction Analysis

The structural phases of pure and Mn^{2+} -doped CdS nanocrystallites were determined by X-ray diffraction pattern. The XRD patterns were recorded twice on two batches of samples for reproducible results. Figure 1 shows the XRD pattern of the as-prepared pure and Mn^{2+} -doped CdS nanocrystallites. The results show a significant amount of line broadening, a characteristic of nanophase materials [31]. The XRD diffraction peaks of pure and Mn^{2+} -doped CdS nanocrystallites reveal that it has a hexagonal phase (JCPDS No. 41-1049) [25, 32]. Additionally, no peaks of impurities were detected, indicating the successful preparation of pure CdS by the simple microwave-assisted combustion method. The observed diffraction peaks at $2\theta = 24.80^\circ$, 26.50° , 28.18° , 43.68° , 47.86° , and 51.82° are associated with (100), (002), (101), (110), (103), and (112) planes, respectively, with the d-spacing values of 0.358, 0.335, 0.316, 0.207, 0.189, and 0.176 nm, respectively. The sharp

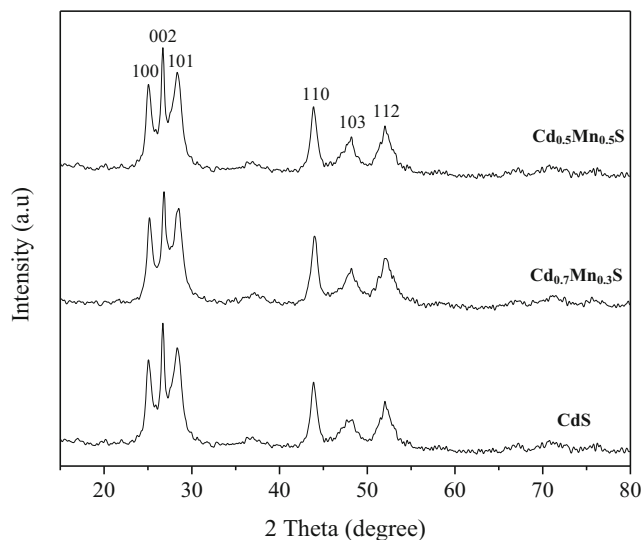


Fig. 1 XRD pattern of CdS ($\text{Mn}_x\text{Cd}_{1-x}\text{S}$: $x = 0.0, 0.3, \text{ and } 0.5$) nanocrystallites

peaks indicate that the pure and Mn^{2+} -doped CdS nanocrystallites possess good crystallinity. The lattice parameters were calculated using the formula [7] given in (1):

$$\sin^2 \theta = \frac{\lambda^2}{4} \left[\frac{4}{3} \left(\frac{h^2 + hk + k^2}{a^2} \right) + \frac{l^2}{c^2} \right] \quad (1)$$

where θ is the diffraction angle; λ , the incident wavelength ($\lambda = 0.1540 \text{ nm}$); and h, k , and l are Miller's indices. The lattice parameter of pure CdS is found to be $a = 4.14 \text{ \AA}$ and $c = 6.71 \text{ \AA}$. Hence, the as-prepared CdS nanocrystallites are determined to be pure hexagonal CdS [25]. Similar results were reported earlier by Kar et al. [32]. However, in the present study, the value of the lattice parameter is reduced with increasing the Mn^{2+} ion content, i.e., $\text{Mn}_{0.5}\text{Cd}_{0.5}\text{S}$ is $a = 4.12 \text{ \AA}$ and $c = 6.69 \text{ \AA}$, thus obeying Vegard's law. The slight decreasing trend in the lattice parameter is attributed to the replacement of larger ionic radius of Cd^{2+} (0.97 \AA) by the smaller ionic radius of Mn^{2+} (0.92 \AA), in the host system [33].

The average crystallite size of pure and Mn^{2+} -doped CdS nanocrystallites was calculated using the Scherrer formula [7] given in (2):

$$L = \frac{0.89\lambda}{\beta \cos \theta} \quad (2)$$

where L is the average crystallite size; λ , the X-ray wavelength; θ , the Bragg diffraction angle; and β , the peak width at half maximum (FWHM). The average crystallite size L calculated from the major diffraction peaks of pure CdS nanocrystallites was found to be in the range of 25.79 nm. It has been observed that the crystallite size is decreased (23.45 and 21.27 nm) with increase the Mn-dopant 0.3 and 0.5 %, respectively. It has a minimum crystallite size of 21.27 nm for 0.5 % Mn concentration, due to the smaller ionic radius of Mn^{2+} ions. Similar results were found by Rahman et al. [33].

3.2 Infrared Spectral Studies

The FT-IR spectrum of pure and Mn^{2+} -doped CdS nanocrystallites are shown in Fig. 2. The spectrum exhibits a common broadband near $3,400 \text{ cm}^{-1}$ due to the OH stretching vibrations of free and hydrogen-bonded hydroxyl groups, and a second typical absorption region at $1,630 \text{ cm}^{-1}$ is assigned to the deformative vibration of water molecules, which is most probably due to water adsorption during the compaction of the powder specimens with KBr [34, 35]. The formation of CdS phase is characterized by an intense and broad IR band with poor resolved shoulders at 626 and $1,120 \text{ cm}^{-1}$ [36, 37].

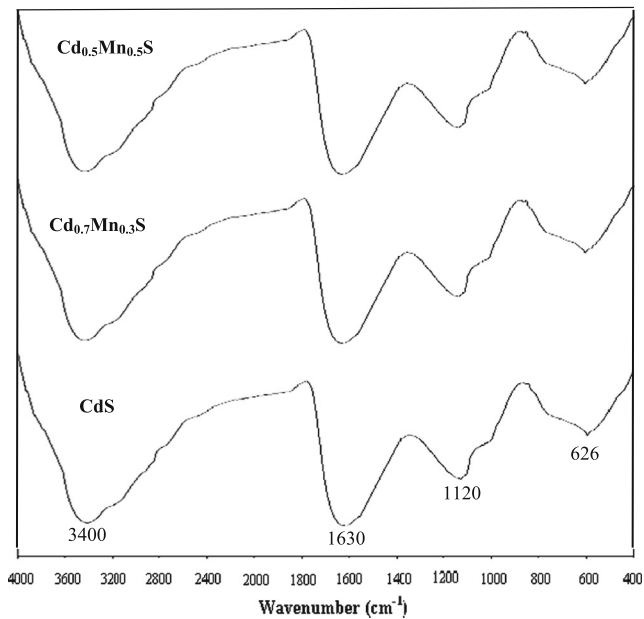
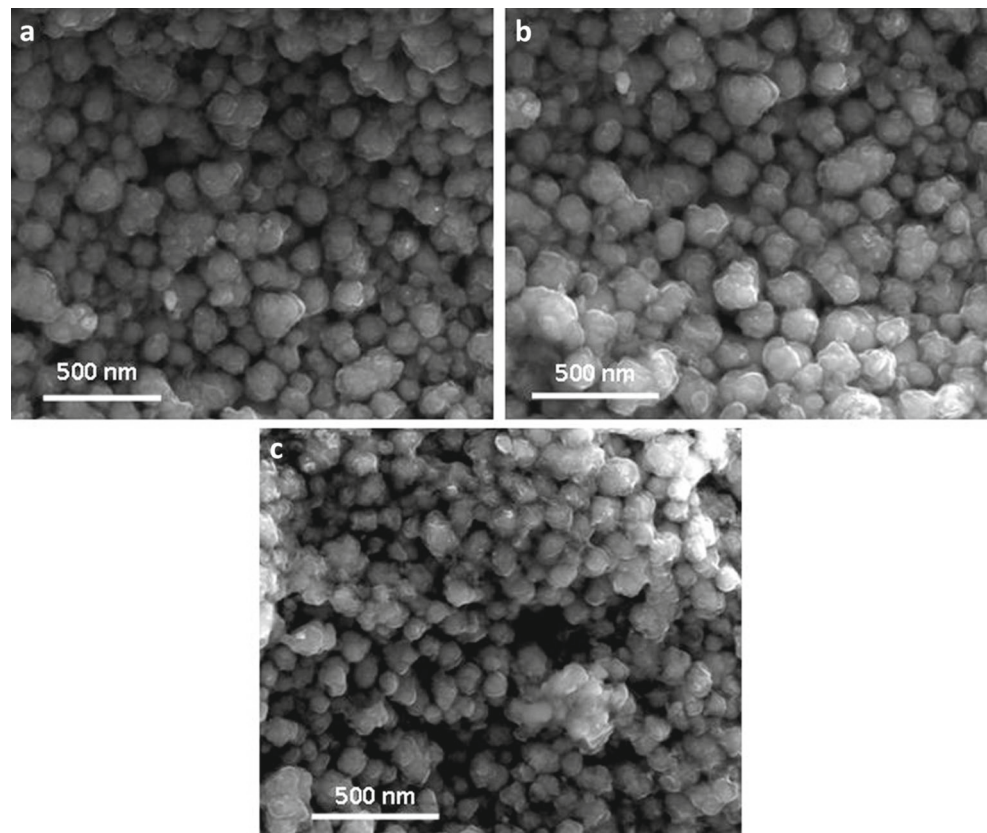


Fig. 2 FT-IR spectra of CdS ($\text{Mn}_x\text{Cd}_{1-x}\text{S}$: $x = 0.0, 0.3,$ and 0.5) nanocrystallites

3.3 SEM Studies

The surface morphology of the as-prepared pure and Mn^{2+} -doped CdS nanocrystallites were examined by HR-SEM studies and are shown in Fig. 3a–c. The HR-SEM

Fig. 3 HR-SEM micrographs of CdS nanocrystallites: **a** CdS, **b** $\text{Mn}_{0.3}\text{Cd}_{0.7}\text{S}$, and **c** $\text{Mn}_{0.5}\text{Cd}_{0.5}\text{S}$ nanocrystallites

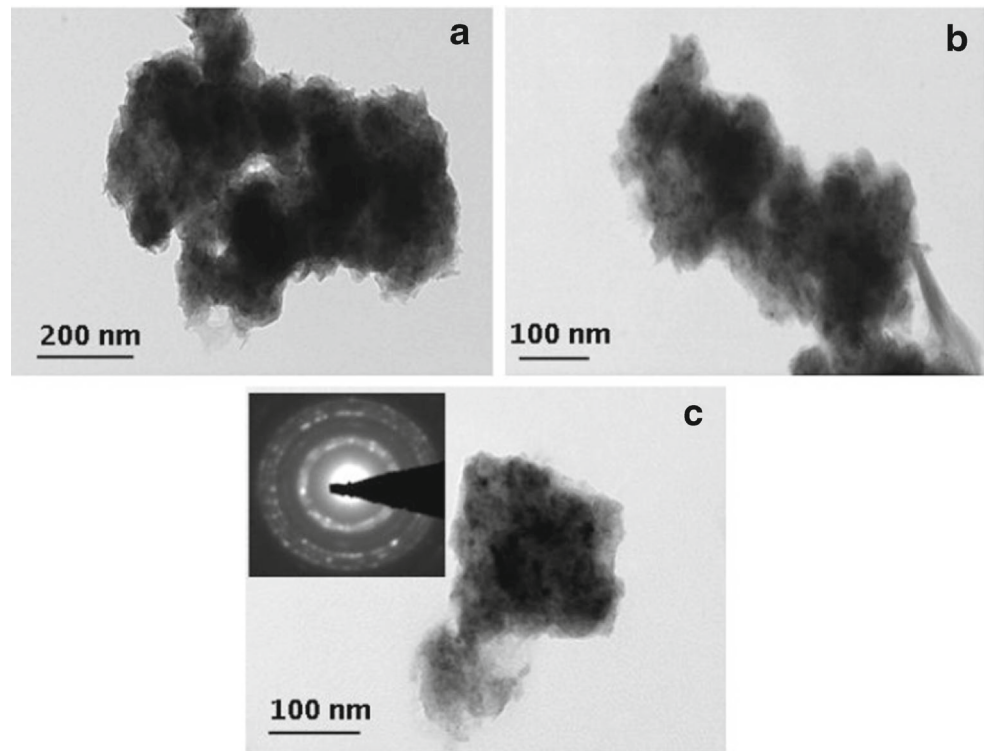


images show the presence of cluster of spherical shaped nanospheres of pure CdS (Fig. 3a), 0.3 % Mn^{2+} -doped CdS (Fig. 3b), and 0.5 % Mn^{2+} -doped CdS crystallites (Fig. 3c), respectively. From the images, it is found that the nanocrystallites are regular in shape and size. It is observed that the particle size of the as-prepared CdS crystallites is decreased with increasing the concentration of Mn^{2+} content. Most of the nanocrystallites are found to be spherical and more evenly dispersed.

3.4 TEM Analysis

In order to investigate the formation of pure and Mn^{2+} -doped CdS nanospheres like cluster structure and to discern whether any secondary phase exist in the samples, a detailed structural characterization was performed by HR-TEM and is shown in Fig. 4a–c. As it can be seen from Fig. 4a, pure CdS nanocrystallite powders derived from microwave-assisted combustion method consist of many spherical shaped domains. Figure 4b, c is a high-magnification image (0.3 and 0.5 % Mn-doped CdS) of spherical sphere joined together, which clearly shows that each of them, belonging to a cluster of nanoparticles, is composed of a number of nanoparticles clustered together at random. These fundamental nanoparticles may contain some defects, due to the microwave vibration frequency, internal stress, and others. These defects are revealed in photoluminescence

Fig. 4 TEM micrographs of CdS nanocrystallites: **a** CdS, **b** $\text{Mn}_{0.3}\text{Cd}_{0.7}\text{S}$, and **c** $\text{Mn}_{0.5}\text{Cd}_{0.5}\text{S}$ nanocrystallites. *Inset of c* shows the corresponding SAED pattern of CdS nanocrystallites



(PL) spectroscopy, which is discussed in Section 3.7. Cd and S sources have an influence on the nucleation and growth of the crystals and will reflect the product morphologies. Apart from the above, crystal growth and morphologies are influenced by the solubility of the precursors in the particular solvent and synthesis conditions [38]. It has been reported [27, 29] that the morphology of the CdS powders obtained in H_2O with cadmium sulfate as precursor shows multiarmed nanorods which is composed by nanocrystallites, while cadmium acetate as a precursor in same H_2O as a solvent using the same microwave solvothermal route shows differently a spherical shaped morphology and are dispersed randomly. Thus, the selection of precursors, solubility of the precursors in the particular solvent, and the synthesis procedure highly influence the morphologies of the nanocrystallites due to the different rates of nucleation and growth. Hence, in the present work, careful selection of precursors, solvent, and synthesis route resulted in the formation of spherical shaped cluster of nanocrystallites. Figure 4c inset displays the corresponding selected area electron diffraction (SAED) pattern of an individual CdS nanosphere with bright concentric rings corresponding to the diffraction planes of the crystalline products. The rings are diffuse and hollow showing that the products are composed of very fine particles, which showed that the nanosphere is polycrystalline. The SAED pattern gives the d-spacing value of 0.35, 0.33, 0.31, 0.20, 0.18, and 0.17

nm, which are consistent with those obtained from XRD data.

3.5 EDX Analysis

The chemical composition of obtained pure and Mn^{2+} -doped nanocrystallites was analyzed by EDX. As shown in Fig. 5a, only Cd and S peaks are present in the spectrum. The results show that the prepared CdS nanocrystallites are elementally pure. As shown in Fig. 5b, only Cd, Mn, and S peaks are present in the spectrum and no other peak is formed. The results show that the as-prepared Mn-doped CdS nanocrystallites are elementally pure.

3.6 Diffuse Reflectance Spectroscopy

The bandgap energy of the obtained pure and Mn^{2+} -doped CdS nanocrystallites was determined from the UV-Visible DRS recorded at room temperature. CdS nanocrystallites absorb light of wavelengths shorter than that of bulk CdS. The optical bandgap (E_g) of pure and Mn^{2+} -doped CdS nanocrystallites can be calculated using the Kubelka-Munk model [7], and the $F(R)$ value is estimated from the following formula given in (3):

$$F(R) = (1 - R)^2/2R \quad (3)$$

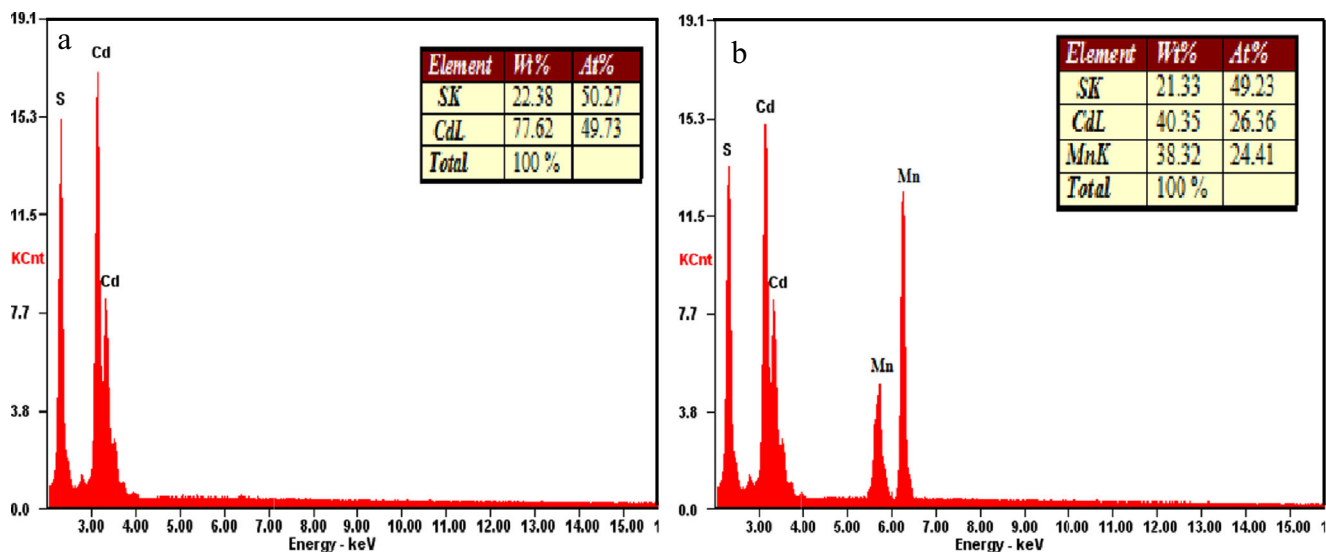
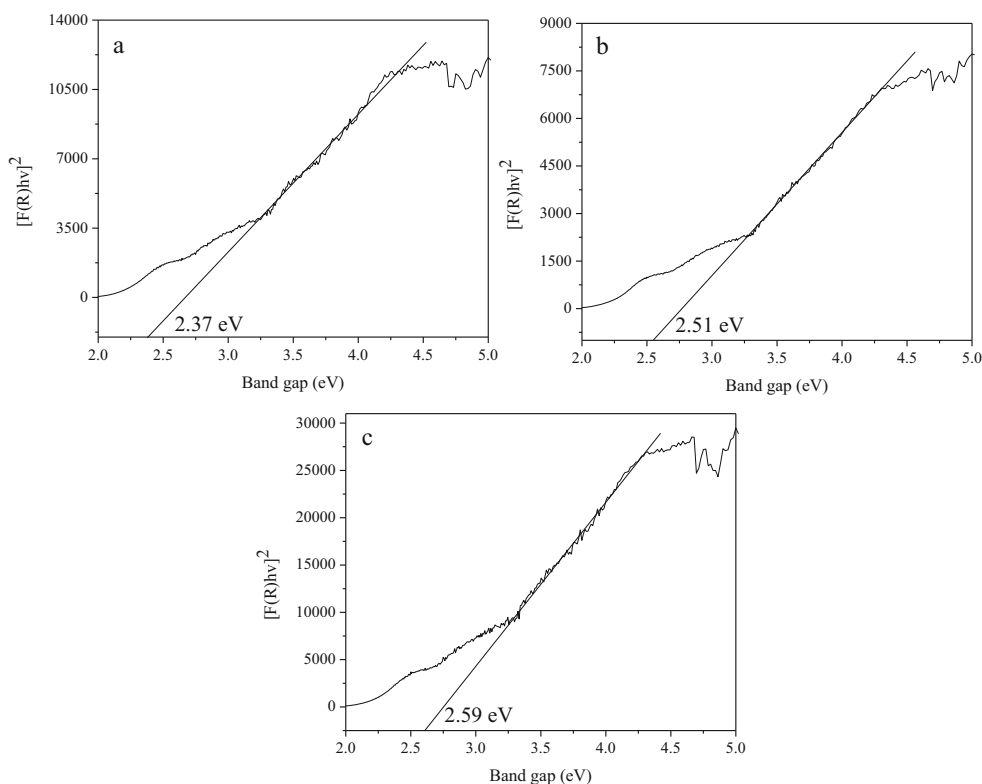


Fig. 5 EDX spectrum of CdS nanocrystallites: **a** CdS and **b** Mn_{0.5}Cd_{0.5}S nanocrystallites

where $F(R)$ is the Kubelka-Munk function, where R is the reflectance. The bandgap can be estimated by extrapolating the linear region of the plot of $[F(R)h\nu]^2$ versus the photon energy as shown in Fig. 6a–c. As the particle size declines, the bandgap increases while the wavelength of absorption shifts to the shorter wavelength [39]. The bandgap of pure CdS nanocrystallites is 2.37 eV, which is calculated from the UV-Visible diffuse reflectance spectra.

The bandgap (E_g) value of bulk CdS is 2.42 eV, and hence, there is a redshift for pure CdS nanocrystallites (2.37 eV) and blueshift for Mn_{0.3}Cd_{0.7}S (2.51 eV) and Mn_{0.5}Cd_{0.5}S (2.59 eV) nanocrystallite samples, which was ascribed to the size quantization. This may be due to the additional sub-bandgap energy levels that are induced by the abundant surface and interface defects in the agglomerated spherical shaped nanospheres of CdS nanocrystallites. The above

Fig. 6 UV-Visible diffuse reflectance spectra of CdS nanocrystallites: **a** CdS, **b** Mn_{0.3}Cd_{0.7}S, and **c** Mn_{0.5}Cd_{0.5}S nanocrystallites



observation indicates that the particle sizes of the CdS nanocrystallites are small and highly crystalline. As already seen from the XRD results, the size of the nanocrystals decreases as the Mn^{2+} -doping concentration is increased. The bandgap of the nanocrystals increases with the decrease in the particle size, due to the quantum confinement effect.

3.7 Photoluminescence Studies

The PL spectra of pure and Mn^{2+} -doped CdS nanocrystallites that are shown in Fig. 7 were recorded for two main reasons: the quantum size effect and structural defects in the crystals. They display two distinct emission bands at approximately 526 nm (green emission, 2.35 eV) with 380 nm of excitation, which were close to those in previous reports for CdS nanoparticles [32, 40]. The band at 526 nm was due to the near band-edge emission. Similar near band-edge emissions from CdS nanostructures were also reported by Kar et al. [32]. The former sharp (band-edge) emission band might be assigned to the electron hole recombination or recombination of the exciton in the mostly delocalized states in nanocrystallites [39, 41]. It indicates the highly crystalline nature of nanocrystallites and the later broad (trap-state) emission might be associated with the trap-state emission, which is due to the defects on the interface between the nanocrystallites and the surrounding medium. It is mainly due to the sulfur vacancies on the surface of the nanocrystallites [39, 41].

The room-temperature PL emission peaks are observed at 572 and 593 nm (orange emissions) in CdS nanocrystallites, which can be attributed to the ${}^4\text{T}_1\text{-}{}^6\text{A}_1$ transition of

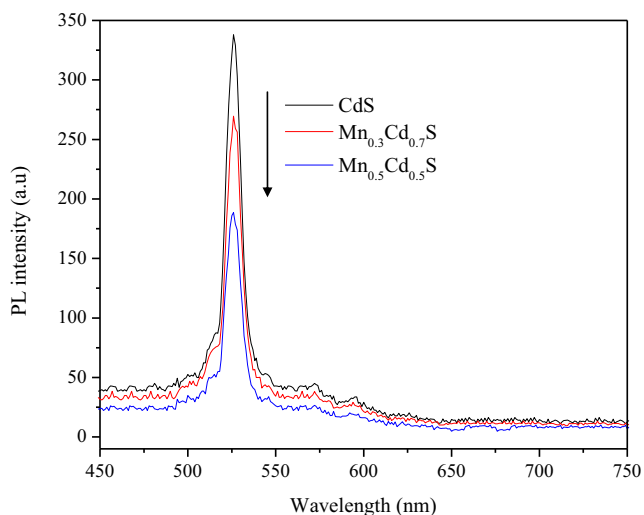


Fig. 7 Room-temperature PL spectra of CdS ($\text{Mn}_x\text{Cd}_{1-x}\text{S}$; $x = 0.0, 0.3, \text{ and } 0.5$) nanocrystallites

the Mn^{2+} ions [42–45]. The decrease in the green emission (526 nm) intensity with increasing the Mn^{2+} content and decrease of crystallite size suggest the presence of various structural defects and the expansion of the bandgap, E_g , thus leading to an increase in the energy variation among the surface states through which the electrons and holes de-excite radiatively. However, dopant metal Mn d levels offer a channel for de-excitation of electrons and holes, other than the surface states. Since the Mn d levels lie in the bandgap region, they can eagerly capture the excited electrons from the band edge as well as surface states [30].

Therefore, it is obvious that when Mn^{2+} -doped CdS nanocrystals are excited, most of the excitation energy is absorbed by the CdS host, and then there is an energy transfer process between the CdS host and the Mn^{2+} ions, which act as the luminescent centers in the CdS host, and finally the orange emission is observed. The results suggest that the energy transfer between the CdS host and the Mn^{2+} impurities is very efficient in Mn^{2+} -doped CdS nanocrystals. It is also observed that the intensity of emission peak decreases with increases in Mn^{2+} . A defect-related red emission was also reported in CdS nanocrystallites [46]. In our present investigations, the absence of such defect-related red emission from the nanocrystals demonstrates that these CdS nanocrystals have excellent optical property and might be used to fabricate photonic devices [32]. As a result, it appears that microwave heating treatment could be an effective tool to control the physicochemical properties of CdS nanocrystallites such as crystal phase (structural), size, morphology, and luminescence, when combined with proper heating treatment and time.

3.8 Vibrating Sample Magnetometer

Figure 8 shows the VSM measurements of pure and Mn-doped CdS nanocrystallites. It denotes the effect of Mn concentrations on magnetic properties of CdS nanocrystallites. The shapes of magnetic hysteresis curves indicate that the diamagnetic signal for pure CdS nanocrystallites and ferromagnetic for Mn-doped CdS nanocrystallites. The observation of ferromagnetic behavior indicates that the Mn^{2+} ions have been substituted the Cd^{2+} sites without changing the hexagonal structure of CdS nanocrystallites. The M-H curves show diamagnetic nature for pure CdS nanocrystallites, and ferromagnetic nature increases with increasing the Mn-doping at room temperature. The value of saturation magnetization (M_s) is increased with increasing the Mn concentrations. The maximum M_s value was found in the sample $\text{Mn}_{0.5}\text{Cd}_{0.5}\text{S}$, among the pure CdS and $\text{Mn}_{0.3}\text{Cd}_{0.7}\text{S}$ nanocrystallites at room temperature. Therefore, we conclude that the observed ferromagnetism at room

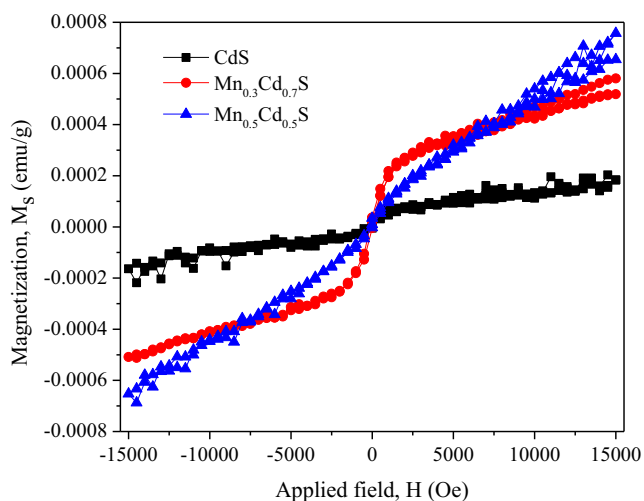


Fig. 8 Magnetic hysteresis loop of CdS ($Mn_xCd_{1-x}S$: $x = 0.0, 0.3$, and 0.5) nanocrystallites

temperature is an intrinsic property, due to the incorporation of Mn into CdS lattice.

The presence of Mn^{2+} ions in the CdS nanocrystals is evidenced from the VSM analysis; thus, one can confidently state that Mn^{2+} ions are present in the nanocrystals [47]. The magnetic properties of the samples can be attributed to the fact that Mn^{2+} ions are present in different environments [48]. Inside the CdS nanocrystals, the Cd^{2+} ions are tetrahedrally coordinated, which can be substituted by Mn^{2+} ions. If Mn^{2+} ions are present on the surface of the CdS nanocrystals, then they would prefer the octahedral coordination. Similar results were reported earlier [48].

The increase in the values of M_s and H_c of the $Cd_{1-x}Mn_xS$ nanocrystallites by increasing the Mn content can be attributed to the magnetic nature of manganese. A similar result was reported earlier [32]. Since the magnetic nature of Mn^{2+} ions ($5 \mu_B$) replaces the nonmagnetic Cd^{2+} ions ($0 \mu_B$) by increasing the composition ($x = 0.3$ and 0.5), hence the values of M_s and the H_c are found to increase with an increase in Mn^{2+} dopant. The sample $Cd_{0.5}Mn_{0.5}S$ shows a higher value of M_s and H_c at room temperature. However, M_s , M_r and H_c values depend on the particle size, crystallinity, nature, and composition of the dopant.

4 Conclusions

CdS nanocrystallites have been successfully synthesized by a simple, rapid, and efficient microwave-assisted combustion method. XRD and FT-IR results were confirmed the formation of CdS phase. It was found that the average size and morphology of CdS nanocrystallites in a sample are dependent on the microwave heating treatment and doping concentration. The formation of spherical shaped cluster of

nanocrystallites is shown by HR-SEM and HR-TEM. The formation of pure CdS is confirmed by EDX. The direct bandgap calculated from UV-Visible diffused reflectance spectra is 2.37 eV, and the synthesized CdS nanocrystallites showed good optoelectronic properties. VSM results of the as-synthesized Mn^{2+} -doped CdS nanocrystallites showed ferromagnetic behavior. It is obvious and interesting to note that the microwave radiation is able to reduce time scales of the reactions and can rapidly lead to very high temperatures which have the influence of accelerating the reaction process, yield, and improvement of the product formation. This synthesis process is an economical and rapid method for the preparation of CdS nanocrystallites with respect to energy, time, and simplicity. Microwave heating treatment is an effective method to control the crystal phase, size, and morphology of CdS nanocrystallites.

Highlights

- Mn^{2+} -doped CdS nanocrystallites were synthesized by microwave-assisted combustion method.
- The as-prepared nanocrystallites have the size of about 40 nm.
- The as-synthesized nanocrystallites were found to have good optical properties.
- Ferromagnetic nature of Mn^{2+} -doped CdS nanocrystallites was confirmed by VSM.

Acknowledgments One of the authors, A. Manikandan is thankful to CSIR, New Delhi, for the award of Senior Research Fellowship (CSIR-SRF).

References

1. Anas, S., Mangalaraja, R.V., Poothayal, M., Shukla, S.K., Ananthakumar, S.: Acta Mater. **55**, 5792 (2007)
2. Koseoglu, Y.: Ceram. Int. **40**, 4673 (2014)
3. Arnold, M.S., Avouris, P., Pan, Z.W., Wang, Z.L.: J. Phys. Chem. B **107**, 659 (2003)
4. Dai, Z.R., Pan, Z.W., Wang, Z.L.: J. Phys. Chem. B **106**, 902 (2002)
5. Ayeshamariam, A., Bououdina, M., Sanjeeviraja, C.: Mater. Sci. Semicon. Proces. **16**, 686 (2013)
6. Lemine, O.M., Sajjeddine, M., Bououdina, M., Msalam, R., Mufti, S., Alyamani, A.: J. Alloys Compd. **502**, 279 (2010)
7. Valan, M.F., Manikandan, A., Arul Antony, S.: J. Nanosci. Nanotech. (2014). Article in press
8. Bae, S.Y., Seo, H.W., Park, J., Yang, H., Park, C., Lee, S.Y.: Appl. Phys. Lett. **81**, 126 (2002)
9. Kar, S., Chaudhuri, S.: J. Phys. Chem. B **109**, 3298 (2005)
10. Dong, L., Jiao, J., Coulter, M., Love, L.: Chem. Phys. Lett. **376**, 653 (2003)
11. Duan, X., Niu, C., Sahi, V., Chen, J., Parce, J.W., Empedocles, S., Goldman, J.L.: Nature **425**, 274 (2003)
12. Liu, Y.K., Zapien, J.A., Geng, C.Y., Shan, Y.Y., Lee, C.S., Lee, S.T.: Appl. Phys. Lett. **85**, 3241 (2004)
13. Zhang, J., Jiang, F.H., Zhang, L.D.: J. Phys. Chem. B **108**, 7002 (2004)
14. Fuhrer, M.S., Nygard, J., Shih, L., Forero, M., Yoon, Y.G., Mazzone, M. S. C., Choi, H.J., Ihm, J., Louie, S.G., Zettl, A., McEuen, P.L.: Science **288**, 494 (2000)

15. Duan, X.F., Huang, Y., Agawal, R., Lieber, C.M.: *Nature* **421**, 241 (2003)
16. Zhan, J.H., Yang, X.G., Wang, D.W., Li, S.D., Xie, Y.T., Xia, Y.N., Qian, Y.T.: *Adv. Mater.* **12**, 1348 (2000)
17. Li, Y., Li, H., Ding, Y., Qian, Y., Yang, L., Zhou, G.: *Chem. Mater.* **10**, 2301 (1998)
18. Yu, S., Wu, Y., Yang, J., Han, Z., Xie, Y., Qian, Y., Liu, X.: *Chem. Mater.* **10**, 2309 (1998)
19. Huang, J., Xie, Y., Li, B., Liu, Y., Qian, Y., Zhang, S.: *Adv. Mater.* **12**, 808 (2000)
20. Xie, Y., Huang, J., Li, B., Liu, Y., Qian, Y.: *Adv. Mater.* **12**, 1523 (2000)
21. Yang, J., Zeng, J., Yu, S., Yang, L., Zhou, G., Qian, Y.: *Chem. Mater.* **12**, 3259 (2000)
22. Li, Y., Wan, J., Gu, Z.: *Mater. Sci. Eng. A* **286**, 106 (2000)
23. Nikirenko, S.I., Koltypin, Y., Mastai, Y., Koltypin, M., Gedanken, A.: *J. Mater. Chem.* **12**, 1450 (2002)
24. Lozovski, V., Strilchuk, G.: *Eur. Phys. J. B* **56**, 297 (2007)
25. Fan, X., Zhang, M.L., Ismathullakhan, S., Zhang, W.J., Lee, C.S., Lee, S.T.: *yst. Growth Des.* **9**, 1375 (2009)
26. Xu, D., Xu, Y., Chen, D., Guo, G., Gui, L., Tang, Y.: *Chem. Phys. Lett.* **325**, 340 (2000)
27. Murugan, A.V., Kale, B.B., Kulkarni, A.V., Kunde, L.B., Saaminathan, V.: *J. Mater. Sci. Mater. Elect.* **16**, 295 (2005)
28. Cao, J.M., Fang, B.Q., Liu, J.S., Chang, S.Q., Zhang, F.: *Chin. J. Inorg. Chem.* **21**, 105 (2005)
29. Thongtema, T., Phuruangrat, A., Thongtem, S.: *J. Phys. Chem. Solids* **69**, 1346 (2008)
30. Nag, A., Sapra, S., Gupta, S.S., Prakash, A., Ghangrekar, A., Periasamy, N., Sarma, D.D.: *Bull. Mater. Sci.* **31**, 561 (2008)
31. Nanda, K.K., Sarangi, S.N., Sahu, S.N.: *Nanostruct. Mater.* **10**, 1401 (1998)
32. Kar, S., Satpati, B., Satyam, P.V., Chaudhuri, S.: *J. Phys. Chem. B* **109**, 19134 (2005)
33. Rahman, S., Nadeem, K., Rehman, M.A., Mumtaz, M., Naeem, S., Papst, I.L.: *Ceram. Int.* **39**, 5235 (2013)
34. Zawrah, M.F.: *Mater. Sci. Eng. A* **382**, 362 (2004)
35. Angappan, S., Bechermans, L.J., Augustine, C.O.: *Mater. Lett.* **58**, 2283 (2004)
36. Wu, Y.D., Wang, L., Xiao, M.W., Huang, X.J.: *J. Non-Cryst. Solids* **354**, 2993 (2008)
37. Feng, M., Chen, Y., Gu, L., He, N., Bai, J., Lin, Y., Zhan, H.: *Eur. Polym. J.* **45**, 1058 (2009)
38. Biswas, S., Kar, S., Chaudhuri, S.: *J. Cryst. Growth* **299**, 94 (2007)
39. Yordanov, G.G., Adachi, E., Dushkin, C.D.: *Mater. Char.* **58**, 267 (2007)
40. Wang, H., Fang, P., Chen, Z., Wang, S.: *J. Alloys Compd.* **461**, 418 (2008)
41. Ramsden, J.J., Webber, S.E., Gratzel, M.: *J. Phys. Chem.* **89**, 2740 (1985)
42. Bol, A.A., Meijerink, A.: *J. Phys. Chem. B* **105**, 10197 (2001)
43. Bol, A.A., Meijerink, A.: *J. Phys. Chem. B* **105**, 10203 (2001)
44. Denzler, D., Olschewski, M., Sattler, K.: *J. Appl. Phys.* **84**, 2841 (1998)
45. Xin, C.L., Hua, Q., Dake, S., Ge, S., Wei, L., Guang, S.Y.: *Sci. China Ser. B Chem.* **52**, 2134 (2009)
46. Wang, Y., Meng, G., Zhang, L., Liang, C., Zhang, J.: *Chem. Mater.* **14**, 1773 (2002)
47. Sapra, S., Nanda, J., Anand, A., Bhat, S.V., Sarma, D.D.: *J. Nanosci. Nanotech.* **3**, 392 (2003)
48. Nag, A., Sapra, S., Nagamani, C., Sharma, A., Pradhan, N., Bhat, S.V., Sarma, D.D.: *Chem. Mater.* **19**, 3252 (2007)